Local momentum and heat fluxes in transient transport processes and inhomogeneous systems

Youping Chen and Adrian Diaz
University of Florida, Department of Mechanical and Aerospace Engineering, Gainesville, Florida 32611, USA
(Received 1 August 2016; revised manuscript received 27 October 2016; published 21 November 2016)

This work examines existing formalisms for the derivation of microscopic momentum and heat fluxes. Both analytical and simulation results are provided to show that the widely used flux formulas are not applicable to transient transport processes or highly inhomogeneous systems, e.g., materials with atomically sharp interfaces. A method is formulated for formally deriving microscopic momentum and heat fluxes through the integral representation of conservation laws. The resulting flux formulas are mathematically rigorous, fully consistent with the physical concepts of momentum and heat fluxes, and applicable to nonequilibrium transient processes in atomically inhomogeneous systems with general many-body forces.

DOI: 10.1103/PhysRevE.94.053309

I. INTRODUCTION

Flux is a basic and ubiquitous concept throughout physics, chemistry, and engineering describing the flow of a physical property in space. The nonequilibrium behavior of transport processes is generally described by transport equations, i.e., conservation equations, in which flux is the measure of transport. The momentum flux measures the rate of momentum transfer across a surface per unit area, while heat flux describes the rate of the conductive flow of internal energy across a surface per unit area. A microscopic definition of flux is required for an atomistic method to calculate a transport property. The objective of this work is twofold: (1) to provide an analysis of why the widely used atomistic formulas for momentum and heat fluxes are not applicable to inhomogeneous systems, and (2) to present a formalism for deriving microscopic momentum and heat fluxes through the integral form of conservation equations.

The paper is structured into four sections. In Sec. II, we examine three main formalisms for deriving momentum and heat fluxes and their applicability. In Sec. III, we present a formalism and derive the atomistic formulas for momentum and heat fluxes. The resulting flux formulas are validated against nonequilibrium molecular dynamics (MD) simulations of the equilibrium state, steady-state heat conduction, and the transient propagation of a heat pulse in a superlattice in Sec. IV. This paper is concluded with a summary and discussions in Sec. V.

II. EXISTING FORMALISMS FOR FLUXES

A. Virial theorem and heat theorem

The virial theorem links the pressure in a many-body system to the kinetic energy and the virial of the potential. It was derived based on a uniform scaling of all particle coordinates [1,2]. By making the shape of the volume, as well as the size, variable [3,4], it can be used to find the average stress of a many-body system under a *uniform* deformation.

A close relative of the "virial theorem" is the "heat theorem." It has been shown that both the virial and heat theorems can be derived based on the fact that the averaged time derivatives of a bounded quantity, $(d/dt)\sum_i \langle m_i \boldsymbol{r}_i \boldsymbol{v}_i\rangle$ or $(d/dt)\sum_i \langle \boldsymbol{r}_i E_i\rangle$, vanishes [3,4]. The formalism leads to a single pressure tensor $\boldsymbol{P}$ and a single heat flux vector $\boldsymbol{Q}$ for the entire system,

$$\boldsymbol{P} = \frac{1}{V}\left\langle \sum_i m_i \boldsymbol{v}_i \boldsymbol{v}_i + \sum_{i<j} \boldsymbol{r}_{ij}\boldsymbol{F}_{ij}\right\rangle, \tag{1}$$

$$\boldsymbol{Q} = \frac{1}{V}\left\langle \sum_i E_i \boldsymbol{v}_i + \frac{1}{2}\sum_{i<j} \boldsymbol{F}_{ij}\boldsymbol{r}_{ij}\cdot(\boldsymbol{v}_i+\boldsymbol{v}_j)\right\rangle, \tag{2}$$

where m_i, $\boldsymbol{r}_i$, $\boldsymbol{v}_i$, E_i are the mass, position, velocity, total energy of the ith particle, respectively, $\boldsymbol{r}_{ij} = \boldsymbol{r}_i - \boldsymbol{r}_j$, $\boldsymbol{F}_{ij}$ is the interparticle force, and V the volume of the system.

Since the virial stress and heat flux are formally written as sums over particles and/or atoms, each individual term in the formulas has been widely used to describe the atomic-scale flux [5]. The applicability of the virial and heat theorems to homogeneous systems (e.g., single crystals in steady-state heat conduction [6,7]) has been demonstrated. However, one can readily see from the formalism that the resulting flux formulas are not applicable to inhomogeneous systems or transient processes where the momentum and heat fluxes may vary on the scale of atomic dimensions.

B. The Irving-Kirkwood formalism

The second formalism was developed by Irving and Kirkwood for their nonequilibrium statistical mechanics formulation of hydrodynamics equations [8], generally referred to as the IK formulation. This formalism uses the infinitely peaked Dirac δ function to define the densities of mass, momentum, and total energy as ensemble averages. Fluxes are then obtained as a result of the differential form of conservation laws. Irving and Kirkwood did not obtain a closed form for the fluxes but expressed them as a power series. The closed-form expressions were obtained later, e.g., by Kreuzer [9], with the difference between two δ functions being expressed as a line integral,

$$\delta(\boldsymbol{r}_k - \boldsymbol{x}) - \delta(\boldsymbol{r}_l - \boldsymbol{x}) = -\nabla_{\boldsymbol{x}}\cdot\boldsymbol{r}_{kl}\int_0^1 \delta(\boldsymbol{r}_k\lambda + \boldsymbol{r}_l(1-\lambda) - \boldsymbol{x})d\lambda. \tag{3}$$

The resulting microscopic stress and heat flux are

$$\bar{\boldsymbol{\sigma}}^{\mathrm{IK}}(\boldsymbol{x},t) = -\left\langle \sum_k m_k \tilde{\boldsymbol{v}}_k \tilde{\boldsymbol{v}}_k \delta(\boldsymbol{r}_k - \boldsymbol{x}) \right\rangle - \left\langle \frac{1}{2}\int_0^1 \sum_{k,l} \boldsymbol{F}_{kl}\boldsymbol{r}_{kl}\delta(\boldsymbol{r}_k\lambda + \boldsymbol{r}_l(1-\lambda) - \boldsymbol{x})d\lambda \right\rangle, \tag{4}$$

$$\bar{\boldsymbol{q}}^{\mathrm{IK}}(\boldsymbol{x},t) = -\left\langle \sum_k \tilde{\boldsymbol{v}}_k \left[\frac{1}{2}m^k(\tilde{\boldsymbol{v}}_k)^2 + \Phi_k\right]\delta(\boldsymbol{r}_k - \boldsymbol{x}) \right\rangle - \left\langle \frac{1}{2}\int_0^1 \sum_{k,l} (\boldsymbol{F}_{kl}\cdot\tilde{\boldsymbol{v}}_k)\boldsymbol{r}_{kl}\delta(\boldsymbol{r}_k\lambda + \boldsymbol{r}_l(1-\lambda) - \boldsymbol{x})d\lambda \right\rangle, \tag{5}$$

where $\tilde{\boldsymbol{v}}_k = \boldsymbol{v}_k - \boldsymbol{v}$ is the difference between the particle velocity and the velocity field. It should be noted that the local densities obtained in the IK formulation are *point functions*, i.e., they are zero everywhere except at the locations of the particles. "These point functions, though averaged neither over space nor time, satisfy equations that are identical in form to the equations of hydrodynamics" [8]. While the point functions reflect the discrete nature of the particle systems, it was noted by Irving and Kirkwood that they must be further averaged in space and time for describing hydrodynamic local properties.

C. Later developments that followed the IK formulation

The methods in the third category are those that average the IK formulation in space for practical applications [10–29]. Except for the *method of planes* that is formulated in reciprocal space and valid for systems with flow in one direction [20–22] and a few generalizations [23,25], the majority of the new developments replaces the infinitely peaked Dirac δ with a continuous weighting function. Noll introduced a probability density function and defined local densities as volume integrals [24]. Hardy employed a localization function Δ[10] and later introduced a bond function $B(k,l,\boldsymbol{x}) = \int_0^1 \Delta[\boldsymbol{r}_k\lambda + \boldsymbol{r}_l(1-\lambda) - \boldsymbol{x}]d\lambda$ for fluxes [12]. The resulting formulas for stress and heat flux are volume averages:

$$\boldsymbol{\sigma}^{\mathrm{Hardy}}(\boldsymbol{x},t) = -\sum_k m_k\tilde{\boldsymbol{v}}_k\tilde{\boldsymbol{v}}_k\Delta(\boldsymbol{r}_k - \boldsymbol{x}) - \frac{1}{2}\sum_{k,l}\boldsymbol{F}_{kl}\boldsymbol{r}_{kl}B(k,l,\boldsymbol{x}), \tag{6}$$

$$\boldsymbol{q}^{\mathrm{Hardy}}(\boldsymbol{x},t) = -\sum_k \tilde{\boldsymbol{v}}_k\left[\frac{1}{2}m_k(\tilde{\boldsymbol{v}}_k)^2 + \Phi_k\right]\Delta(\boldsymbol{r}_k - \boldsymbol{x}) - \frac{1}{2}\sum_{k,l}(\boldsymbol{F}_{kl}\cdot\tilde{\boldsymbol{v}}_k)\boldsymbol{r}_{kl}B(k,l,\boldsymbol{x}). \tag{7}$$

Numerous formulations have further followed the work by Noll or that by Hardy and obtained volume-averaged formulas similar in structure to these in Eqs. (6) and (7).

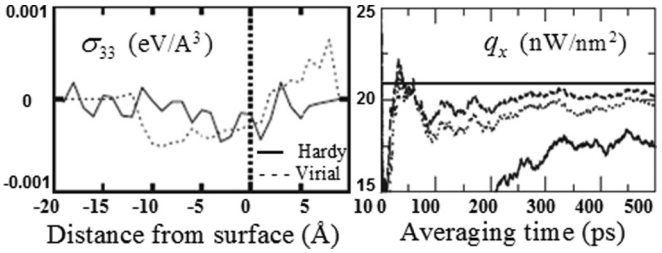

FIG. 1. Left: Hardy and virial stress at zero temperature and pressure at and away from a free surface [31]. Right: Heat flux using Hardy's formula as a function of averaging time computed by averaging over 2 (solid), 6 (dotted), and 10 (dashed) volume elements whose radius is 1.0 nm. The horizontal line is the prescribed value of the heat flux [32].

D. An analysis of the volume-averaging methods

Comparing the formulas obtained from the three formalisms, it can be seen that there are two commonalities. First, both $\boldsymbol{\sigma}$ and $\boldsymbol{q}$ contain two parts, the kinetic part due to the motion of individual particles, and the potential part due to the interaction between particles. The kinetic parts from all three methods are similar, except for a few erroneous formulations in the literature. Second, if the size of the averaging volume exceeds the cutoff of the interparticle potential, the volume-averaged fluxes become identical in form to the fluxes defined in Eqs. (1) and (2). This is consistent with various computational results demonstrating that fluxes calculated using different formulas are similar when a sufficiently large volume is used [30–33]; with a smaller averaging volume they are different from each other and from the prescribed values of fluxes [31–34]; cf. Fig. 1.

It is for inhomogeneous systems that different formalisms lead to different values of the fluxes. The major departure of the later developments from the original IK formalism is to average the IK formulas over a volume element without distinguishing densities that are defined per unit volume with fluxes that are defined per unit area. This incurs the following consequences.

(1) Although for homogenous systems the calculated fluxes, if averaged over a large volume and a long time interval, may converge [31–33], they do not converge to the prescribed fluxes for inhomogeneous systems [34].

(2) The formula for the potential part of momentum flux is commonly interpreted in terms of the dyadic products, $\boldsymbol{F}_{ij}\boldsymbol{r}_{ij}$, and for the potential part of heat flux in terms of the triple products, $\boldsymbol{F}_{ij}\cdot\boldsymbol{v}_i\boldsymbol{r}_{ij}$. This leads to various misinterpretations such as "the microscopic stress is symmetric" [35] and "the potential heat flux is the rate at which particle i is doing work on particle j, multiplied by the distance over which this energy is transferred" [36].

(3) The potential part of momentum flux does not have the fundamental properties of Cauchy stress: (a) The Cauchy stress vectors acting on the opposite sides of a surface at a given point are equal in magnitude and opposite in sign, and (b) the Cauchy stress vector acting on any plane at a point can be determined by the normal vector to the plane and the Cauchy stress tensor at the same point. Without these two properties, the stress formulas cannot be used to predict the critical value

of the stress vector on a specific plane such as a cleavage or a slip plane.

(4) The volume-averaged flux formulas have also deviated from the physical concept of heat flux as the rate of heat flow through a surface per unit area. Without the size and the orientation of the "surface" in the atomistic definition of the flux, the formulas cannot be used to find the heat flux at a given surface such as an oriented phase interface or a grain boundary.

III. A DIFFERENT FORMULATION

A. The averaging method

The IK formalism employs the Dirac δ to link a local density to its corresponding phase function. To define a continuum field quantity, the IK point functions, i.e., the infinitely peaked Dirac δ, must be averaged in space and time. In this work, we derive three types of integrations of the Dirac δ to link a phase function to a field quantity. For local densities that are localized at a point due to the properties of individual particles, we define an averaged Dirac δ over a volume element $V(\boldsymbol{x})$ of volume V as

$$\bar{\delta}_V(\boldsymbol{r}_k-\boldsymbol{x}) \equiv \frac{1}{V}\iiint_{V(\boldsymbol{x})}\delta(\boldsymbol{r}_k-\boldsymbol{x}')d^3x' = \begin{cases}1/V, & \text{if } \boldsymbol{r}_k\in V(\boldsymbol{x}),\\ 0, & \text{otherwise.}\end{cases} \tag{8}$$

The microscopic expressions of fluxes that arise from the interaction forces between particles involve the difference between two Dirac δ functions. In our previous work [37], we have shown that the difference between two Dirac δ functions can be expressed using the fundamental theorem for line integrals as

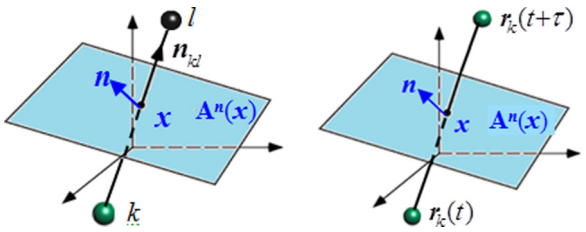

FIG. 2. Line $\boldsymbol{L}_{kl}$ in space (left) and path $\boldsymbol{r}_k$ in time (right) intersect with the surface element $\boldsymbol{A}^n(\boldsymbol{x})$.

$$\delta(\boldsymbol{r}_k-\boldsymbol{x})-\delta(\boldsymbol{r}_l-\boldsymbol{x}) = \int_{\boldsymbol{L}_{lk}}\nabla_{\boldsymbol{\varphi}}\delta(\boldsymbol{\varphi}-\boldsymbol{x})\cdot d\boldsymbol{\varphi} = \nabla_{\boldsymbol{x}}\cdot\int_{\boldsymbol{L}_{kl}}\delta(\boldsymbol{\varphi}-\boldsymbol{x})d\boldsymbol{\varphi}, \tag{9}$$

where $\boldsymbol{L}_{lk}$ represents a line segment from $\boldsymbol{r}_l$ to $\boldsymbol{r}_k$, and $\boldsymbol{L}_{kl}$ represents a line segment from $\boldsymbol{r}_k$ to $\boldsymbol{r}_l$; cf. Fig. 2. Denote $\boldsymbol{n}_{kl}=(n_{kl}^x,n_{kl}^y,n_{kl}^z)=n_{kl}^\alpha\boldsymbol{e}^\alpha$ as the unit direction vector of $\boldsymbol{L}_{kl}$ and introduce a scale ϕ such that $\boldsymbol{\varphi}-\boldsymbol{r}_k=\lambda(\boldsymbol{r}_l-\boldsymbol{r}_k)=\phi\boldsymbol{n}_{kl}$; the line integral can be parametrized by

$$\int_{\boldsymbol{L}_{kl}}\delta(\boldsymbol{\varphi}-\boldsymbol{x})d\boldsymbol{\varphi}=\boldsymbol{n}_{kl}\int_0^{|\boldsymbol{r}_{kl}|}\delta(\phi\boldsymbol{n}_{kl}+\boldsymbol{r}_k-\boldsymbol{x})d\phi. \tag{10}$$

To measure the interaction forces between particles on opposite sides of a surface element, the line integral needs to be integrated over the surface element. For this purpose, let us first consider a coordinate surface element $\boldsymbol{A}^z(\boldsymbol{x})$, centered at $\boldsymbol{x}=(x,y,z)$, with normal along the coordinate axis $\boldsymbol{e}^z$ and area A^z. Using the sifting and the scaling properties of the Dirac δ, $\int_{a-\varepsilon}^{a+\varepsilon}f(x)\delta(x-c)dx=f(c)$ and $\delta(cx)=\delta(x)/|c|$, the area-averaged line integral of the Dirac δ over a coordinate surface element $\boldsymbol{A}^z(\boldsymbol{x})$ can be expressed as

$$\begin{aligned}\int_{\boldsymbol{L}_{kl}}\bar{\delta}_A^z(\boldsymbol{\varphi}-\boldsymbol{x})d\boldsymbol{\varphi} &\equiv \frac{1}{A^z}\iint_{\boldsymbol{A}^z(\boldsymbol{x})}d\boldsymbol{A}\cdot\int_{\boldsymbol{L}_{kl}}\delta(\boldsymbol{\varphi}-\boldsymbol{x}')d\boldsymbol{\varphi}=\frac{\boldsymbol{e}^z\cdot\boldsymbol{n}_{kl}}{A^z}\iint_{\boldsymbol{A}^z(\boldsymbol{x})}dx'dy'\int_0^{|\boldsymbol{r}_{kl}|}\delta(\phi\boldsymbol{n}_{kl}+\boldsymbol{r}_k-\boldsymbol{x}')d\phi\\ &=\frac{n_{kl}^z}{A^z}\iint_{\boldsymbol{A}^z}dx'dy'\int_0^{|\boldsymbol{r}_{kl}|}\delta\big(\phi n_{kl}^x+r_k^x-x'\big)\delta\big(\phi n_{kl}^y+r_k^y-y'\big)\delta\big(\phi n_{kl}^z+r_k^z-z'\big)d\phi\\ &=\frac{n_{kl}^z}{A^z\big|n_{kl}^xn_{kl}^yn_{kl}^z\big|}\iint_{\boldsymbol{A}^z(\boldsymbol{x})}\delta\left(\frac{r_k^z-z'}{n_{kl}^z}-\frac{r_k^x-x'}{n_{kl}^x}\right)\delta\left(\frac{r_k^z-z'}{n_{kl}^z}-\frac{r_k^y-y'}{n_{kl}^y}\right)dx'dy'\\ &=\frac{1}{A^z}\frac{n_{kl}^z}{\big|n_{kl}^z\big|}\begin{cases}1, & \text{if } \boldsymbol{x}\in\boldsymbol{A}^z \text{ and } \boldsymbol{x}\in[\boldsymbol{r}_k\boldsymbol{r}_l],\\ 0, & \text{otherwise.}\end{cases}\end{aligned} \tag{11}$$

The differential surface element $d\boldsymbol{A}$ can be represented using indicial notation as $d\boldsymbol{A}=\boldsymbol{n}dA=n^\alpha\boldsymbol{e}^\alpha dA=\boldsymbol{e}^\alpha dA^\alpha$, where $\alpha(\alpha=1,2,3\text{ or }x,y,z)$ is a summation index. The area-averaged line integral of the Dirac δ over an arbitrary surface element $\boldsymbol{A}^n(\boldsymbol{x})$ can then be expressed as

$$\begin{aligned}\int_{\boldsymbol{L}_{kl}}\bar{\delta}_A^n(\boldsymbol{\varphi}-\boldsymbol{x})d\boldsymbol{\varphi} &\equiv \frac{1}{A^n}\iint_{A^n(\boldsymbol{x})}d\boldsymbol{A}\cdot\int_{\boldsymbol{L}_{kl}}\delta(\boldsymbol{\varphi}-\boldsymbol{x}')d\boldsymbol{\varphi}\\ &=\frac{1}{A^n}\iint_{A^\alpha(\boldsymbol{x})}\boldsymbol{e}^\alpha dA^\alpha\cdot\int_{\boldsymbol{L}_{kl}}\delta(\boldsymbol{\varphi}-\boldsymbol{x}')d\boldsymbol{\varphi}=\frac{A^\alpha}{A^n}\int_{\boldsymbol{L}_{kl}}\bar{\delta}_A^\alpha(\boldsymbol{\varphi}-\boldsymbol{x})d\boldsymbol{\varphi}=n^\alpha\int_{\boldsymbol{L}_{kl}}\bar{\delta}_A^\alpha(\boldsymbol{\varphi}-\boldsymbol{x})d\boldsymbol{\varphi}.\end{aligned} \tag{12}$$

The integrals in Eq. (12) can also be evaluated using the line-plane intersection theorem together with the defining properties of Dirac δ: $\delta(\boldsymbol{x}) = 0$ for $\boldsymbol{x} \neq 0$ and $\int_V \delta(\boldsymbol{x})dV = 1$. The intersection of a line and a plane can be the empty set, a point, or a line. The value of the integrals is zero if the intersection is the empty set; otherwise, it is unity. In the case that the intersection is a line, the integrals in Eq. (11) can be evaluated by taking the limit as $n^z_{kl} \to 0$. The significance of Eq. (12) is that it relates the area-averaged line integral of the Dirac δ over an arbitrary surface element to that over three coordinate surface elements.

The transfer of momentum and heat across a surface also occurs through the motion of particles; this can also be described as a line-plane intersection problem; cf. Fig. 2. Since it takes a finite time for a particle to reach and cross a surface, and also since in atomistic simulations the equation of motion is solved step-by-step in discrete time intervals, we define an area-time-averaged Dirac δ over a coordinate surface element $\boldsymbol{A}^z(\boldsymbol{x})$ and a time-step interval T as

$$\begin{aligned}\bar{\delta}^z_{AT}(\boldsymbol{r}_k - \boldsymbol{x}) &\equiv \frac{1}{A^z T}\iint_{\boldsymbol{A}^z(\boldsymbol{x})} d\boldsymbol{A}\int_0^T \delta(\boldsymbol{r}_k(t+\tau) - \boldsymbol{x}')d\tau \\ &= \frac{\boldsymbol{e}^z}{A^z T}\iint_{\boldsymbol{A}^z(\boldsymbol{x})} d^2x'\int_0^T \delta(\boldsymbol{r}_k(t) + \boldsymbol{v}_k\tau - \boldsymbol{x}')d\tau \\ &= \begin{cases}\frac{\boldsymbol{e}^z}{A^z T|v^z_k|}, & \text{if } \boldsymbol{r}_k(t+\tau) \in \boldsymbol{A}^z(\boldsymbol{x}) \text{ for } \tau \in T, \\ 0, & \text{otherwise.}\end{cases}\end{aligned} \tag{13}$$

Equation (13) can be generalized to arbitrarily oriented surface element. Denote $\boldsymbol{n}$ as the normal of a surface element, it can be shown that $\bar{\delta}^n_{AT}(\boldsymbol{r}_k - \boldsymbol{x}) = n^\alpha \bar{\delta}^\alpha_{AT}(\boldsymbol{r}_k - \boldsymbol{x})$.

In summary, we have derived a volume-integrated Dirac δ, $\bar{\delta}_V(\boldsymbol{r}_k - \boldsymbol{x})$, for local densities that are measured per unit volume and an area-line-integrated Dirac δ, $\int_{L_{kl}} \bar{\delta}^n_A(\boldsymbol{\varphi} - \boldsymbol{x})$, as well as an area-time-integrated Dirac δ, $\bar{\delta}^n_{AT}(\boldsymbol{r}_k - \boldsymbol{x})$, for fluxes that are measured per unit area and time, with $\int_{L_{kl}} \bar{\delta}^n_A(\boldsymbol{\varphi} - \boldsymbol{x}) = \int_{L_{kl}} \bar{\delta}^n_{AT}(\boldsymbol{\varphi} - \boldsymbol{x})$ when T is a time-step interval. It should be noted that the Dirac δ was defined by Dirac through integration [38]. It does not itself have a definite value. Only triple integrals of a three-dimensional Dirac δ are well defined and hence can provide the unique link between a field quantity and a phase function through the sifting property. Further averaging a field quantity in space or time shall not change the microscopic expression of the field quantity. In distinction from volume-averaging methods that assume somewhat arbitrary weighting functions, in this work the link is defined through integrating the Dirac δ.

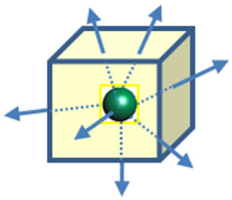

FIG. 3. Internal forces in $V(\mathbf{x})$ and surface forces on ∂V.

B. Microscopic momentum flux

The mass density (mass per unit volume) can be defined using Eq. (8) as

$$\begin{aligned}\rho(\boldsymbol{x},t) &\equiv \frac{1}{V}\iiint_{V(\boldsymbol{x})}\sum_k m_k\delta(\boldsymbol{r}_k - \boldsymbol{x}')d^3x' \\ &\equiv \sum_k m_k\bar{\delta}_V(\boldsymbol{r}_k - \boldsymbol{x}).\end{aligned} \tag{14}$$

Consequently, the momentum density $\rho\boldsymbol{v}$ is also a volume average and may be further averaged over a time-step interval T for the description of the flow of momentum across a surface per unit area per unit time at point $\boldsymbol{x}$ and time t,

$$\rho\boldsymbol{v}(\boldsymbol{x},t) \equiv \frac{1}{T}\int_0^T d\tau\frac{1}{V}\iiint_{V(\boldsymbol{x})}\sum_k m_k\boldsymbol{v}_k\delta(\boldsymbol{r}_k - \boldsymbol{x}')d^3x'. \tag{15}$$

There are two types of forces acting on the volume element $V(\boldsymbol{x})$: forces exerted on $V(\boldsymbol{x})$ from external sources, and forces exerted on $V(\boldsymbol{x})$ by the surrounding material as a result of the interaction between particles inside and outside of $V(\boldsymbol{x})$. An important fact is that the total internal force in $V(\boldsymbol{x})$ is equal to the total force acting on the enclosing surface ∂V; Fig. 3.

In the absence of external forces, the momentum conservation equation can be derived using Newton's second law and expressed in terms of two surface integrals as

$$\begin{aligned}\frac{\partial}{\partial t}(\rho\boldsymbol{v}) &\equiv \frac{\partial}{\partial t}\left\{\frac{1}{T}\int_0^T d\tau\frac{1}{V}\iiint_{V(\boldsymbol{x})}\sum_k m_k\boldsymbol{v}_k\delta(\boldsymbol{r}_k - \boldsymbol{x}')d^3x'\right\} \\ &= \frac{1}{TV}\int_0^T d\tau\iiint_{V(\boldsymbol{x})}\left\{\sum_k m_k\dot{\boldsymbol{v}}_k\delta(\boldsymbol{r}_k - \boldsymbol{x}') + \sum_k m_k\boldsymbol{v}_k\frac{\partial}{\partial t}\delta(\boldsymbol{r}_k - \boldsymbol{x}')\right\}d^3x' \\ &= \frac{1}{TV}\int_0^T d\tau\iiint_{V(\boldsymbol{x})}\left\{\sum_{k,l}\boldsymbol{F}_{kl}\delta(\boldsymbol{r}_k - \boldsymbol{x}') - \nabla_{\boldsymbol{x}'}\cdot\sum_k m_k\boldsymbol{v}_k\boldsymbol{v}_k\delta(\boldsymbol{r}_k - \boldsymbol{x}')\right\}d^3x' \\ &= \frac{1}{V}\iint_{\partial V}\boldsymbol{t}dA - \frac{1}{TV}\int_0^T d\tau\iint_{\partial V}\sum_k m_k\tilde{\boldsymbol{v}}_k\boldsymbol{v}_k\delta(\boldsymbol{r}_k - \boldsymbol{x}')\cdot\boldsymbol{n}dA + \frac{1}{V}\iint_{\partial V}\rho\boldsymbol{v}\boldsymbol{v}\cdot\boldsymbol{n}dA \\ &\equiv \frac{1}{V}\iint_{\partial V}\boldsymbol{\sigma}_{\text{pot}}\cdot\boldsymbol{n}dA + \frac{1}{V}\iint_{\partial V}(\boldsymbol{\sigma}_{\text{kin}} - \rho\boldsymbol{v}\boldsymbol{v})\cdot\boldsymbol{n}dA,\end{aligned} \tag{16}$$

where $\boldsymbol{\sigma}_{\text{kin}}$ and $\boldsymbol{\sigma}_{\text{pot}}$ are the kinetic and potential momentum flux across ∂V; $\boldsymbol{t}$ is the surface traction at a point of ∂V due to the interaction force between particles on opposite sides of ∂V; $\boldsymbol{t} = \boldsymbol{\sigma}_{\text{pot}} \cdot \boldsymbol{n}$ or $t^\alpha = \sigma^{\alpha\beta} n^\beta$, with $\boldsymbol{n}$ being the surface normal. The time-step-averaged stress vector can then be obtained using Eqs. (12) and (16) as

$$\begin{aligned}\boldsymbol{t}(\boldsymbol{x},\boldsymbol{n}) &= \sum_{k<l} \boldsymbol{F}_{kl} \int_{\boldsymbol{L}_{kl}} \bar{\delta}_A^n(\boldsymbol{\varphi}-\boldsymbol{x})d\boldsymbol{\varphi} \\ &= n^\beta \sum_{k<l} \boldsymbol{F}_{kl} \int_{\boldsymbol{L}_{kl}} \bar{\delta}_A^\beta(\boldsymbol{\varphi}-\boldsymbol{x})d\boldsymbol{\varphi}. \end{aligned} \tag{17}$$

It follows

$$\boldsymbol{\sigma}_{\text{pot}}(\boldsymbol{x},t) = \sum_{k<l} F_{kl}^\alpha \int_{\boldsymbol{L}_{kl}} \bar{\delta}_A^\beta(\boldsymbol{\varphi}-\boldsymbol{x})d\boldsymbol{\varphi}\boldsymbol{e}^\alpha\boldsymbol{e}^\beta, \tag{18}$$

in which, according to Eq. (11),

$$F_{kl}^\alpha \int_{\boldsymbol{L}_{kl}} \bar{\delta}_A^\beta(\boldsymbol{\varphi}-\boldsymbol{x})d\boldsymbol{\varphi} = \frac{F_{kl}^\alpha}{A^\beta} \begin{cases} 1, & \text{if } r_{kl} \text{ intersects } \boldsymbol{A}^\beta(\boldsymbol{x}) \text{ and } \boldsymbol{e}^\beta \cdot \boldsymbol{n}_{kl} \geqslant 0, \\ -1, & \text{if } r_{kl} \text{ intersects } \boldsymbol{A}^\beta(\boldsymbol{x}) \text{ and } \boldsymbol{e}^\beta \cdot \boldsymbol{n}_{kl} < 0, \\ 0, & \text{otherwise.} \end{cases}$$

Equation (18) indicates $\sigma_{\text{pot}}^{\alpha\beta}(\boldsymbol{x},t)$ is the αth component of the forces per unit area per unit time transmitting through the βth coordinate plane at point $\boldsymbol{x}$, with α being the direction of the forces and β the normal of the coordinate plane. Thus, the potential part of momentum flux defined in Eq. (18) is identical to the mechanical stress.

Equation (16) also uniquely defines $\boldsymbol{\sigma}_{\text{kin}}$. As a result of Eq. (16) holding for any ∂V,

$$\begin{aligned}&\frac{1}{TA_\beta}\int_0^T d\tau \iint_{\boldsymbol{A}^\beta} \sum_k m_k \tilde{\boldsymbol{v}}_k \boldsymbol{v}_k \delta(\boldsymbol{r}_k - \boldsymbol{x}') \cdot \boldsymbol{e}^\beta dA \\ &\quad = -\frac{1}{A_\beta}\iint_{\boldsymbol{A}^\beta} \boldsymbol{\sigma}_{\text{kin}} \cdot \boldsymbol{e}^\beta dA. \end{aligned} \tag{19}$$

When T is a time-step interval, we have

$$\boldsymbol{\sigma}_{\text{kin}}(\boldsymbol{x},t) = \sigma_{\text{kin}}^{ab}\boldsymbol{e}^\alpha\boldsymbol{e}^\beta = -\sum_k m_k \tilde{\boldsymbol{v}}_k v_k^\beta \bar{\delta}_{AT}^\beta(\boldsymbol{r}_k - \boldsymbol{x}), \tag{20}$$

in which, according to Eq. (13),

$$m_k \tilde{\boldsymbol{v}}_k v_k^\beta \bar{\delta}_{AT}^\beta(\boldsymbol{r}_k - \boldsymbol{x}) = \frac{m_k \tilde{v}_k^\alpha \boldsymbol{e}^\alpha \boldsymbol{e}^\beta}{A^\beta T} \begin{cases} 1, & \text{if } \boldsymbol{r}_k \text{ intersects } A^\beta(\boldsymbol{x}) \text{ and } \boldsymbol{e}^\beta \cdot \boldsymbol{v}_k \geqslant 0, \\ -1, & \text{if } \boldsymbol{r}_k \text{ intersects } A^\beta(\boldsymbol{x}) \text{ and } \boldsymbol{e}^\beta \cdot \boldsymbol{v}_k < 0, \\ 0, & \text{otherwise.} \end{cases}$$

This means that the kinetic momentum flux $\sigma_{\text{kin}}^{\alpha\beta}$ is the relative momentum across a surface per unit area and per unit time with respect to the velocity field, with α being the direction of the momentum and β the normal of the coordinate plane. Combining Eqs. (18) and (20), we obtain the atomistic formula for momentum flux measured per unit area at point $\boldsymbol{x}$ and time t as a time-step-interval average as

$$\begin{aligned}\boldsymbol{\sigma}(\boldsymbol{x},t) = &-\sum_k m_k \tilde{v}_k^\alpha v_k^\beta \boldsymbol{e}^\alpha \bar{\delta}_{AT}^\beta(\boldsymbol{r}_k - \boldsymbol{x}) \\ &+ \sum_{k<l} F_{kl}^\alpha \int_{\boldsymbol{L}_{kl}} \bar{\delta}_A^\beta(\boldsymbol{\varphi}-\boldsymbol{x})d\boldsymbol{\varphi}\boldsymbol{e}^\alpha\boldsymbol{e}^\beta. \end{aligned} \tag{21}$$

Equation (21) is valid for any additive potential. For a specific potential function, the interaction force $\boldsymbol{F}_{kl}$ can be derived in terms of the total energy or the site energies [6,39]. For example, for the general form of many-body potentials, $\Phi = \sum_{ij}\Phi_2(\boldsymbol{r}_{ij}) + \sum_{ijk}\Phi_3(\boldsymbol{r}_{ij},\boldsymbol{r}_{ik}) + \sum_{ijkn}\Phi_4(\boldsymbol{r}_{ij},\boldsymbol{r}_{ik},\boldsymbol{r}_{in}) + \cdots = \sum_i \Phi_i$, there are the following equivalent expressions for $\boldsymbol{F}_{kl}$:

$$\boldsymbol{F}_{kl} = -\frac{\partial\Phi}{\partial\boldsymbol{r}_{kl}} = -\frac{\partial(\Phi_l+\Phi_k)}{\partial\boldsymbol{r}_{kl}} = -\left(\frac{\partial\Phi_l}{\partial\boldsymbol{r}_k} - \frac{\partial\Phi_k}{\partial\boldsymbol{r}_l}\right) = -\boldsymbol{F}_{lk}. \tag{22}$$

Substituting $\boldsymbol{F}_{kl}$ in Eq. (22) into Eq. (21) and using the summation index interchange, the atomistic momentum flux can then be expressed in terms of site potential energies as

$$\begin{aligned}\boldsymbol{\sigma}(\boldsymbol{x},t) = &-\sum_k m_k \tilde{v}_k^\alpha \tilde{v}_k^\beta \boldsymbol{e}^\alpha \bar{\delta}_{AT}^\beta(\boldsymbol{r}_k - \boldsymbol{x}) \\ &- \sum_{k,l} \frac{\partial\Phi_l}{\partial r_k^\alpha} \int_{\boldsymbol{L}_{kl}} \bar{\delta}_A^\beta(\boldsymbol{\varphi}-\boldsymbol{x})d\boldsymbol{\varphi}\boldsymbol{e}^\alpha\boldsymbol{e}^\beta. \end{aligned} \tag{23}$$

It is noticed that the momentum flux formula in Eq. (23) is formally different from the existing volume-averaged microscopic formula for stress. A different derivation that averages the IK point functions to obtain the potential part of stress and a discussion on the equivalence of the atomistic and Cauchy stress can be found in Ref. [37], in which the same potential stress formula is obtained.

C. Microscopic heat flux

Similarly, the integral form of the energy conservation equation over the volume element $V(\boldsymbol{x})$ and over a time-step interval T can be expressed as

$$\begin{aligned}\frac{\partial}{\partial t}(\rho E) &\equiv \frac{\partial}{\partial t}\left\{\frac{1}{T}\int_0^T d\tau \frac{1}{V}\iiint_{V(\boldsymbol{x})} \sum_k E_k \delta(\boldsymbol{r}_k - \boldsymbol{x}')\right\} d^3x' \\ &= \frac{1}{T}\int_0^T d\tau \frac{1}{V}\iiint_{V(\boldsymbol{x})} \left\{\sum_k \dot{E}_k \delta(\boldsymbol{r}_k - \boldsymbol{x}') - \nabla_{\boldsymbol{x}'} \cdot \sum_k E_k \delta(\boldsymbol{r}_k - \boldsymbol{x}')\boldsymbol{v}_k\right\} d^3x' \\ &\equiv \frac{1}{V}\iint_{\partial V} (\boldsymbol{q}_{\text{pot}} + \boldsymbol{\sigma}_{\text{pot}} \cdot \boldsymbol{v}) \cdot d\boldsymbol{A} + \frac{1}{V}\iint_{\partial V} (\boldsymbol{q}_{\text{kin}} + \boldsymbol{\sigma}_{\text{kin}} \cdot \boldsymbol{v} - \rho E \boldsymbol{v}) \cdot d\boldsymbol{A}, \end{aligned} \tag{24}$$

in which the two surface integrals represent the potential and kinetic energy flow across the enclosing surface ∂V per unit time. Since Eq. (24) is valid for any arbitrary ∂V, $\frac{1}{T}\int_0^T d\tau \iint_A \sum_k E_k \tilde{\boldsymbol{v}}_k \bar{\delta}_T(\boldsymbol{r}_k - \boldsymbol{x}') \cdot \boldsymbol{n} dA = -\iint_A (\boldsymbol{q}_{\rm kin} + \boldsymbol{\sigma}_{\rm kin} \cdot \boldsymbol{v}) \cdot \boldsymbol{n} dA$ must hold for any coordinate surface element. As a result,

$$\boldsymbol{q}_{\rm kin} + \boldsymbol{\sigma}_{\rm kin} \cdot \boldsymbol{v} = -\sum_k \left(\frac{1}{2} m_k \tilde{\boldsymbol{v}}_k^2 + \Phi_k + m_k \boldsymbol{v}_k \cdot \boldsymbol{v}\right) \tilde{v}_k^\alpha \bar{\delta}_{AT}^\alpha(\boldsymbol{r}_k - \boldsymbol{x}). \tag{25}$$

The potential energy flux can also be identified using Eq. (24) and can be further derived in terms of particle site energies using Newton's second law and force theorem. Note that

$$\begin{aligned}
&\iiint_{V(\boldsymbol{x})} d^3x' \sum_k \dot{E}_k \delta(\boldsymbol{r}_k - \boldsymbol{x}') \\
&= \iiint_{V(\boldsymbol{x})} d^3x' \sum_k [m_k \boldsymbol{v}_k \cdot \dot{\boldsymbol{v}}_k + \dot{\Phi}_k] \delta(\boldsymbol{r}_k - \boldsymbol{x}') \\
&= \iiint_{V(\boldsymbol{x})} d^3x' \sum_{k,l} \left\{ -\frac{\partial \Phi_l}{\partial \boldsymbol{r}_k} \cdot \boldsymbol{v}_k + \frac{\partial \Phi_k}{\partial \boldsymbol{r}_l} \cdot \boldsymbol{v}_l \right\} \delta(\boldsymbol{r}_k - \boldsymbol{x}') \\
&= -\iiint_{V(\boldsymbol{x})} d^3x' \sum_{k,l(\neq k)} \frac{\partial \Phi_l}{\partial \boldsymbol{r}_k} \cdot \boldsymbol{v}_k \left(\delta(\boldsymbol{r}_k - \boldsymbol{x}) - \delta(\boldsymbol{r}_l - \boldsymbol{x}')\right) \\
&= \iint_{\partial V} \sum_{k,l(\neq k)} \frac{\partial \Phi_l}{\partial \boldsymbol{r}_k} \cdot \boldsymbol{v}_k \int_{\boldsymbol{L}_{kl}} \delta(\boldsymbol{\varphi} - \boldsymbol{x}') d\boldsymbol{\varphi} \cdot \boldsymbol{n} d^2x'
\end{aligned} \tag{26}$$

is valid for arbitrary ∂V. Thus

$$\boldsymbol{q}_{\rm pot} + \boldsymbol{\sigma}_{\rm pot} \cdot \boldsymbol{v} = \sum_{k,l(\neq k)} \frac{\partial \Phi_l}{\partial \boldsymbol{r}_k} \cdot \boldsymbol{v}_k \int_{\boldsymbol{L}_{kl}} \bar{\delta}_{AT}^\alpha(\boldsymbol{\varphi} - \boldsymbol{x}) \, d\boldsymbol{\varphi} \boldsymbol{e}^\alpha. \tag{27}$$

Substituting $\boldsymbol{\sigma}_{\rm kin}$ and $\boldsymbol{\sigma}_{\rm pot}$ in Eq. (23) into Eqs. (25) and (27) and combining $\boldsymbol{q}_{\rm pot}$ and $\boldsymbol{q}_{\rm kin}$, we obtain the heat flux as

$$\begin{aligned}
\boldsymbol{q}(\boldsymbol{x},t) = &-\sum_k \tilde{v}_k^\alpha \left[\frac{1}{2} m^k (\tilde{\boldsymbol{v}}_k)^2 + \Phi_k\right] \bar{\delta}_{AT}^\alpha(\boldsymbol{r}_k - \boldsymbol{x}) \\
&+ \sum_{k,l(\neq k)} \frac{\partial \Phi_l}{\partial \boldsymbol{r}_k} \cdot \tilde{\boldsymbol{v}}_k \int_{\boldsymbol{L}_{kl}} \bar{\delta}_{AT}^\alpha(\boldsymbol{\varphi} - \boldsymbol{x}) d\boldsymbol{\varphi} \boldsymbol{e}^\alpha.
\end{aligned} \tag{28}$$

It is seen that our heat flux formula is also formally and fundamentally different from the volume-averaged formulas for heat flux. The kinetic part is the internal energy across a surface per unit time and area through the microscopic thermal motion of particles. The potential part of heat flux is the work done per unit area and time by the interaction forces between particles on the opposite of the surface through the microscopic thermal motion of the particles. This is in sharp distinction from the interpretation by volume-averaging methods as "the rate of work done multiplied by the distance over which this energy is transferred." Also, as illustrated in Fig. 4, the αth component of the heat flux vector at point $\boldsymbol{x}$ is the energy transferred across the αth coordinate plane at $\boldsymbol{x}$, whereas it is the αth component of $\boldsymbol{r}_{ij}$ (the distance between two particles) in the volume-averaging formulations.

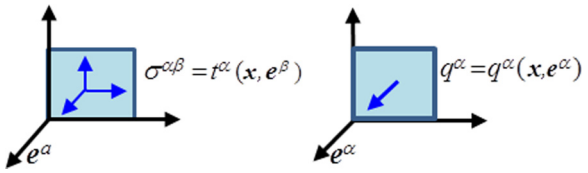

FIG. 4. Illustration of the association of the components of stress and heat flux with the coordinate surfaces.

IV. A COMPARISON OF MD RESULTS OF HEAT FLUX USING DIFFERENT FORMULAS

To provide a quantitative understanding of the consequence of the formal difference between heat flux formulas, we simulate a superlattice structure consisting of alternating layers of two different materials and atomically flat coherent phase interfaces, as shown in Fig. 5. The two materials have a face-centered-cubic structure with lattice constant $a = 2.628$ Å. The LJ (Lennard-Jones) potential is used to describe the interaction between atoms in both materials, with a mass of 47.98 g/mol, $\epsilon_{11} = 0.0104$ eV, and $\sigma_{11} = 3.4$ Å for the atoms in the red region, while a mass of 39.95 g/mol, $\epsilon_{22} = 0.0520$ eV, and $\sigma_{22} = 3.4$ Å for the blue region. The LJ interaction between the two regions uses $\epsilon_{12} = 0.0233$ eV and $\sigma_{12} = 3.4$ Å. The length of the simulation cell is 1000 Å with a cross section of 29×29 Å. The model is intended for the measurement of one-dimensional transport and is periodic in all directions.

The equilibrium state, steady-state heat conduction, and the transient propagation of a heat pulse in a superlattice are simulated using MD. The heat flux in the simulations is measured using three completely different formulas:

(1) *Surface*: the surface-averaged heat flux formulas defined in Eqs. (25), (27), and (28), with which the fluxes are calculated locally in term of the positions and velocities of atoms.

(2) *Volume*: the volume-averaged energy flux formula defined in Eq. (2), which is the heat flux formula implemented in the large-scale stomic/molecular massively parallel simulator (LAMMPS) and widely used in equilibrium MD simulations.

(3) *Continuum*: the energy flux formula derived based on the hydrodynamics continuity equation through measuring the change of the total energy in a region to quantify the flow

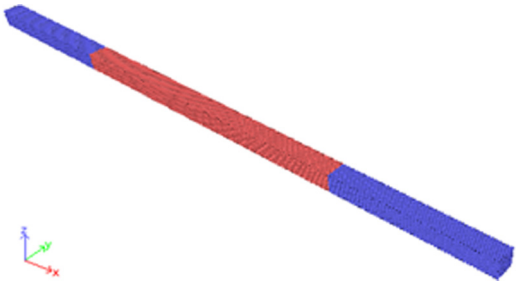

FIG. 5. MD model of a superlattice.

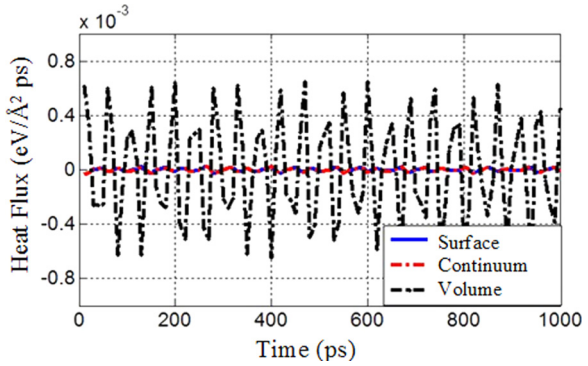

FIG. 6. Heat flux at an interface in the equilibrium state averaged over a time interval of 10 000 fs. The volume used for the volume-averaged formula is 29 × 29 × 20 Å.

of energy across the entire surface enclosing the region. This is the formula used in nonequilibrium MD simulations with the heat-source-sink scheme to calculate the heat flux in one-dimensional (1D) steady-state heat conduction [40–43]. It was also used in the "method of plane" and was called "mesoscopic derivation because it does not explicitly refer to molecular quantities" [21]. Note that this is not a local heat flux formula and cannot be used to find a local heat flux. It is used in this work to calculate the energy flux across two symmetrically located interfaces.

In Fig. 6 we plot the MD simulation result of the heat flux as a function of time in the equilibrium state under zero temperature, zero pressure. It is seen from Fig. 6 that both the surface formula and the continuum formula accurately reproduce the prescribed zero heat flux. By contrast, the volume formula significantly overestimates the heat flux at the interface. After averaging over a large volume and a large time interval, pronounced oscillations are still present in the computed heat flux by the volume formula. This result is in agreement with other computational findings in the literature [31–34].

In Fig. 7 we plot the steady-state heat conduction simulation results as a function of time. The prescribed value of the heat flux is 5.2×10^{-5} eV/Å^{2}ps. It is seen from Fig. 7 that the surface formula is able to reproduce the prescribed value of

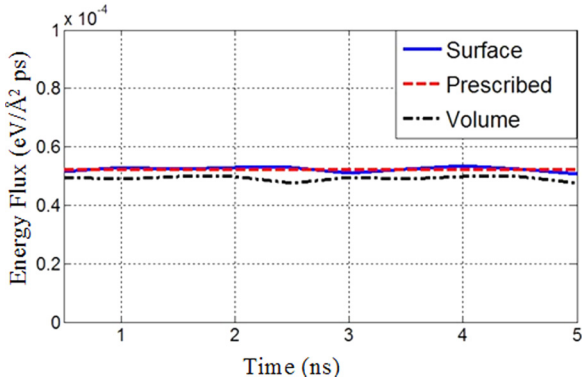

FIG. 7. Heat flux at an interface in the steady-state heat conduction averaged over a time interval of 500 ps. The volume used for the volume-averaged formula is 29 × 29 × 2.8 Å.

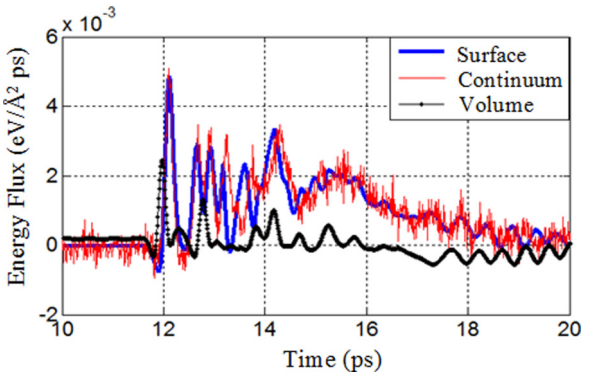

FIG. 8. Energy flux in the heat pulse simulation averaged over time intervals of 10 fs and over the two interfaces in Fig. 5. The volume used with the volume formula is 29 × 29 × 4 Å. The heat pulse is applied in the middle of the specimen at time zero for 2 fs. There is a high-frequency noise present in the continuum signal most likely due to the finite time step used in its computation.

heat flux, but the volume formula underestimates the heat flux at the phase interface.

The transient heat pulse simulation results are plotted in Fig. 8. To compare with the continuum formula that can only calculate the average energy flux through the two symmetrically located interfaces in Fig. 5, the energy flux is calculated locally at each interface using the surface formula and then averaged over the two interfaces. It is seen from Fig. 8 that the time-dependent energy flux at the interfaces predicted by the surface formulas compares well with that by the continuum formula during the propagation of the heat pulse. The volume formula, on the other hand, significantly underestimates the transient energy flux. It is evident that the volume formula is incapable of describing transient energy flux across the interfaces.

To summarize the three sets of MD simulation results, the volume formula of heat flux fails to reproduce the prescribed heat flux in the equilibrium and steady-state simulations of the superlattice and significantly underestimates energy flux in the transient simulation; the surface formula, on the other hand, is shown to reproduce the heat flux prescribed in the equilibrium and steady-state simulations and produce the same time history of the heat flux as the continuum formula in the transient heat pulse propagation simulation. The applicability of our heat flux formulas, as well as the inapplicability of the volume-averaged heat flux formulas, to nonequilibrium inhomogeneous systems is thus demonstrated.

V. SUMMARY AND DISCUSSIONS

In this work we have formulated a method for formally deriving microscopic expressions for momentum and heat fluxes. Differing from the IK formalism that uses the differential form of conservation equations, our method derives the flux formulas from the integral representation of conservation laws. The formulation naturally leads to the expressions of fluxes as a measure of the flow of a physical property through a surface per unit area per unit time. Consequently, it removes the ambiguity associated with the vanishing divergence of fluxes in the differential form of conservation laws.

In distinction from the volume-averaging approaches that avoid the use of the Dirac δ function, this work takes advantage of the rigorous mathematical concept of the Dirac δ. We distinguish local densities that are measured per unit volume with fluxes that are measured per unit area and time. In addition, we use the fundamental theorem for line integrals to express the difference between two Dirac δ functions. This facilitates the mathematical representation of the fluxes across a surface as a line-plane intersection problem. The resulting atomistic formulas for fluxes are fully consistent with the field concepts of momentum and heat fluxes, valid for systems with general additive many-body potentials, and applicable to both equilibrium state and transient thermal transport processes in homogeneous or atomically inhomogeneous systems.

It is noticed that our formulas for local momentum and heat flux can be reduced to the flux formulas derived using the "method of planes" for systems with flow in one direction [20–22]. However, our flux formulas are formally and fundamentally different from those obtained using virial or heat theorems or through volume averaging the IK point functions. The physical concept of fluxes as the rate of transfer of a physical property through a surface is simple and applicable at all scales. The IK formulation is valid at the atomic scale. It is averaging the IK point function over a finite-sized volume that makes the volume-averaged formulas incapable of describing fluxes in inhomogeneous systems. Although the volume-averaged flux formulas remain valid for homogeneous systems such as gaseous systems or single crystals in equilibrium or in steady states, they become invalid for transient processes or for solid materials that involve microstructural discontinuities, such as defects, material phase interfaces, grain boundaries in polycrystalline materials, etc. The applicability of these heat flux formulas, as well as the inapplicability of the existing volume-averaged heat flux formulas, to inhomogeneous systems are demonstrated through nonequilibrium MD simulations of the heat flux in a superlattice.

In the landmark paper, Irving and Kirkwood assumed, for the purpose of mathematical simplicity, a single component and single phase system composed of point molecules with the internal degrees of freedom being ignored. The formulation of this work, as well as the IK formulation, can be extended to a two-level structural description of polyatomic materials by including the internal degrees of freedom within molecules or unit cells [18]. A crystalline (or a molecular) material is then viewed as a continuous collection of lattice cells but embedded within each lattice cell is a group of discrete atoms. In that case, the volume element that contains only one atom should be replaced by one that contains more than one atom but one lattice point, whereas the smallest volume of the volume elements is still that of the primitive unit cell, with which the volume elements can completely fill the space the material occupies and, in the absence of external forces, the distribution of local densities are continuous and homogeneous from the atomic to the macroscopic scale.

ACKNOWLEDGMENTS

This material is based upon research supported by the U.S. Department of Energy, Office of Basic Energy Sciences, Division of Materials Sciences and Engineering under Award No. DE-SC0006539. Discussion with Professor James Dufty on this work is gratefully acknowledged.

[1] O. Nielsen and R. M. Martin, Quantum-mechanical theory of stress and force, Phys. Rev. B **32**, 3780 (1985).
[2] V. Fock, Bemerkung zum virialsatz, Z. Phys. **63**, 855 (1930).
[3] W. G. Hoover, *Computational Statistical Mechanics* (Elsevier, Amsterdam, 1991).
[4] W. G. Hoover, *Molecular Dynamics*, Lecture Notes in Physics Vol. 258 (Springer, Berlin, 1986).
[5] K. S. Cheung and S. Yip, Atomic-level stress in an inhomogeneous system, J. Appl. Phys. **70**, 5688 (1991).
[6] Z. Fan, L. F. C. Pereira, H. Q. Wang, J. C. Zheng, D. Donadio, and A. Harju, Force and heat current formulas for many-body potentials in molecular dynamics simulations with applications to thermal conductivity calculations, Phys. Rev. B **92**, 094301 (2015).
[7] R. E. Jones and D. K. Ward, Estimates of crystalline LiF thermal conductivity at high temperature and pressure by a Green-Kubo method, Phys. Rev. B **94**, 014309 (2016).
[8] J. Irving and J. G. Kirkwood, The statistical mechanical theory of transport processes. IV. The equations of hydrodynamics, J. Chem. Phys. **18**, 817 (1950).
[9] H. J. Kreuzer, *Nonequilibrium Thermodynamics and Its Statistical Foundations* (Clarendon, Oxford, U.K., 1981).
[10] R. J. Hardy, Energy-flux operator for a lattice, Phys. Rev. **132**, 168 (1963).
[11] J. K. Flicker and P. L. Leath, Thermal conductivity in high-concentration mixed crystals, Phys. Rev. B **7**, 2296 (1973).
[12] R. J. Hardy, Formulas for determining local properties in molecular-dynamics simulations: Shock waves, J. Chem. Phys. **76**, 622 (1982).
[13] Y. Chen and J. D. Lee, Connecting molecular dynamics to micromorphic theory. (I). Instantaneous and averaged mechanical variables, Physica A **322**, 359 (2003).
[14] Y. Chen and J. D. Lee, Connecting molecular dynamics to micromorphic theory. (II). Balance laws, Physica A **322**, 377 (2003).
[15] J. Z. Yang, X. Wu, and X. Li, A generalized Irving-Kirkwood formula for the calculation of stress in molecular dynamics models, J. Chem. Phys. **137**, 134104 (2012).
[16] R. B. Lehoucq and M. P. Sears, Statistical mechanical foundation of the peridynamic nonlocal continuum theory: Energy and momentum conservation laws, Phys. Rev. E **84**, 031112 (2011).
[17] Y. Chen, Local stress and heat flux in atomistic systems involving three-body forces, J. Chem. Phys. **124**, 054113 (2006).
[18] Y. Chen, Reformulation of microscopic balance equations for multiscale materials modeling, J. Chem. Phys. **130**, 134706 (2009).
[19] S. Lepri, R. Livi, and A. Politi, Thermal conduction in classical low-dimensional lattices, Phys. Rep. **377**, 1 (2003).

[20] J. Zhang and B. Todd, Pressure tensor and heat flux vector for inhomogeneous nonequilibrium fluids under the influence of three-body forces, Phys. Rev. E **69**, 031111 (2004).
[21] B. Todd, P. J. Daivis, and D. J. Evans, Heat flux vector in highly inhomogeneous nonequilibrium fluids, Phys. Rev. E **51**, 4362 (1995).
[22] B. D. Todd, D. J. Evans, and P. J. Daivis, Pressure tensor for inhomogeneous fluids, Phys. Rev. E **52**, 1627 (1995).
[23] H. Heinz, W. Paul, and K. Binder, Calculation of local pressure tensors in systems with many-body interactions, Phys. Rev. E **72**, 066704 (2005).
[24] R. B. Lehoucq and A. Von Lilienfeld-Toal, Translation of Walter Noll's "Derivation of the fundamental equations of continuum thermodynamics from statistical mechanics," J. Elasticity **100**, 5 (2010).
[25] M. Han and J. S. Lee, Method for calculating the heat and momentum fluxes of inhomogeneous fluids, Phys. Rev. E **70**, 061205 (2004).
[26] X. Li, Heat conduction in nanoscale materials: A statistical-mechanics derivation of the local heat flux, Phys. Rev. E **90**, 032112 (2014).
[27] E. Smith, D. Heyes, D. Dini, and T. Zaki, Control-volume representation of molecular dynamics, Phys. Rev. E **85**, 056705 (2012).
[28] Y. Chen and J. Lee, Atomistic formulation of a multiscale field theory for nano/micro solids, Philos. Mag. **85**, 4095 (2005).
[29] Y. Chen, J. Zimmerman, A. Krivtsov, and D. L. McDowell, Assessment of atomistic coarse-graining methods, Int. J. Eng. Sci. **49**, 1337 (2011).
[30] D. Tsai, The virial theorem and stress calculation in molecular dynamics, J. Chem. Phys. **70**, 1375 (1979).
[31] J. A. Zimmerman *et al.*, Calculation of stress in atomistic simulation, Modell. Simul. Mater. Sci. Eng. **12**, S319 (2004).
[32] E. B. Webb, J. A. Zimmerman, and S. C. Seel, Reconsideration of continuum thermomechanical quantities in atomic scale simulations, Math. Mech. Solids **13**, 221 (2008).
[33] J. Cormier, J. Rickman, and T. Delph, Stress calculation in atomistic simulations of perfect and imperfect solids, J. Appl. Phys. **89**, 99 (2001).
[34] T. J. Delph, Local stresses and elastic constants at the atomic scale, Proc. R. Soc. London, Ser. A **461**, 1869 (2005).
[35] A. I. Murdoch, *Physical Foundations of Continuum Mechanics* (Cambridge University Press, Cambridge, U.K., 2012).
[36] P. B. Allen and J. L. Feldman, Thermal conductivity of disordered harmonic solids, Phys. Rev. B **48**, 12581 (1993).
[37] Y. Chen, The origin of the distinction between microscopic formulas for stress and Cauchy stress, arXiv:1609.02491.
[38] P. Dirac, *The Principles of Quantum Mechanics* (Oxford University Press, Oxford, U.K., 1930).
[39] V. A. Kuzkin, Interatomic force in systems with multibody interactions, Phys. Rev. E **82**, 016704 (2010).
[40] Z. Zheng *et al.*, Phonon thermal transport through tilt grain boundaries in strontium titanate, J. Appl. Phys. **116**, 073706 (2014).
[41] W. Li, X. Chen, Z. Zheng, and Y. Chen, Minimum thermal conductivity in periodically twinned $SrTiO_3$, Comput. Mater. Sci. **112**, 107 (2016).
[42] T. Zhu and E. Ertekin, Phonon transport on two-dimensional graphene/boron nitride superlattices, Phys. Rev. B **90**, 195209 (2014).
[43] T. Zhu and E. Ertekin, Resolving anomalous strain effects on two-dimensional phonon flows: The cases of graphene, boron nitride, and planar superlattices, Phys. Rev. B **91**, 205429 (2015).